

**Linking the Eta Model with the Community Multiscale Air Quality (CMAQ) Modeling
System to Build a National Air Quality Forecasting System**

Tanya L. Otte^{1*}, George Pouliot¹, Jonathan E. Pleim¹, Jeffrey O. Young¹, Kenneth L. Schere¹,
David C. Wong², Pius C. S. Lee³, Marina Tsidulko³, Jeffery T. McQueen⁴,
Paula Davidson⁵, Rohit Mathur¹, Hui-Ya Chuang³, Geoff DiMego⁴, and Nelson L. Seaman⁵

Final draft for *Weather and Forecasting*

3 December 2004

¹ Atmospheric Sciences Modeling Division, Air Resources Laboratory, National Oceanic and Atmospheric Administration, Research Triangle Park, North Carolina. (On assignment to the National Exposure Research Laboratory, U.S. Environmental Protection Agency.)

² Lockheed Martin Information Technology, Research Triangle Park, North Carolina.

³ Science Applications International Corporation, Camp Springs, Maryland.

⁴ National Centers for Environmental Prediction, Camp Springs, Maryland.

⁵ Office of Science and Technology, National Weather Service, Silver Spring, Maryland.

* *Corresponding author address:* Tanya L. Otte, NOAA/ARL/ASMD, U.S. EPA Mail Drop E243-03, Research Triangle Park, NC 27711. E-mail: *tanya.otte@noaa.gov*

Abstract

NOAA and the United States Environmental Protection Agency (EPA) have developed a national air quality forecasting (AQF) system that is based on numerical models for meteorology, emissions, and chemistry. The AQF system generates gridded model forecasts of ground-level ozone (O_3) that can help air quality forecasters to predict and alert the public of the onset, severity, and duration of poor air quality conditions. Although AQF efforts have existed in metropolitan centers for many years, this AQF system provides a national numerical guidance product and the first-ever air quality forecasts for many (predominantly rural) areas of the United States.

Currently, the AQF system is based on NCEP's Eta Model and the EPA's Community Multiscale Air Quality (CMAQ) Modeling System. The AQF system, which was implemented into operations at the NWS in September 2004, currently generates twice-daily forecasts of O_3 for the northeast United States at 12-km horizontal grid spacing. Preoperational testing to support the 2003 and 2004 O_3 forecast seasons showed that the AQF system provided valuable guidance that could be used in the air quality forecast process. The AQF system will be expanded over the next several years to include a nationwide domain, a capability for forecasting fine particle pollution, and a longer forecast period. State and local agencies will now issue air quality forecasts that are based, in part, on guidance from the AQF system. This paper describes the process and software components used to link the Eta Model and CMAQ for the national AQF system, discusses several technical and logistical issues that were considered, and provides examples of O_3 forecasts from the AQF system.

1. Introduction

Since the late 1990s, deterministic, coupled meteorology-chemistry modeling systems have been adapted and refined for air quality forecasting (AQF) purposes. McHenry et al. (1999, 2004) developed an air chemistry prediction system based on coupling the Fifth-Generation Penn State/National Center for Atmospheric Research (NCAR) Mesoscale Model (MM5; Grell et al. 1994) and the Multiscale Air Quality Simulation Platform–Real Time (MAQSIP–RT). Grell et al. (2000) developed an online system where MM5 is coupled with an embedded chemistry model (MM5-Chem). Stein et al. (2000) use a hybrid Eulerian-Lagrangian photochemical forecasting system where MM5 output is linked to the Hybrid Single-Particle Lagrangian Integrated Trajectory Model (HYSPLIT) to forecast O₃. A handful of other similar modeling efforts exist within the research and forecast communities (e.g., Flato et al. 2000; Lawrence et al. 2003; Uno et al. 2003; Vaughn et al. 2004; Cope et al. 2004). McHenry et al. (2004), using an example from the 2001 forecasting season, show that deterministic AQF systems have comparable or better skill than other AQF methods (cf. EPA 1999a).

On 6 May 2003, the National Oceanic and Atmospheric Administration (NOAA) and the United States Environmental Protection Agency (EPA) formally signed a Memorandum of Understanding and a Memorandum of Agreement to expand their collaboration toward the development of a national AQF system. NOAA and the EPA have the common objective to conduct research and operations in the coupling of meteorology and air chemistry to develop and use state-of-the-science operational air quality models. NOAA and the EPA have jointly developed various components of the AQF system. The models run operationally at the NOAA's National Weather Service (NWS) to provide air quality forecast guidance for the United States. The EPA interprets and disseminates the forecast information from a public health perspective [e.g., via the Air Quality Index (AQI); see Table 1] as well as provides source emissions and air monitoring data to NOAA for use in operational modeling and evaluation. The state and local agencies which have historically provided air quality forecasts now provide local AQI forecasts and warnings based, in part, on the national guidance products from the AQF

system. Figure 1 shows the roles of NOAA, the EPA, and the state and local agencies in the partnership to implement the AQF system.

Although the EPA's National Ambient Air Quality Standards (NAAQS) exist for several criteria pollutants, much of the poor air quality during the summer in the northeast United States is linked to ozone (O_3) (e.g., Wolff and Liroy 1978; Ryan et al. 2000). Tropospheric O_3 is formed from chemical reactions between volatile organic compounds (VOCs) and nitrogen oxides (NO_x) that occur in heat and sunlight. The precursors of O_3 are found in motor vehicle exhaust, emissions from industry and electric utilities, gasoline vapors, chemical solvents, and vegetation. Exposure to high concentrations of O_3 can trigger health problems and can damage plants and ecosystems. Harmful concentrations of near-surface O_3 typically originate in and most often affect urban areas, but rural areas can be impacted because of long-range pollutant transport. Harmful O_3 concentrations are typically observed during hot, dry, stagnant conditions. The peak O_3 concentrations are often observed near the time of the maximum surface temperature for urban areas that are not located in high terrain. Concentrations of O_3 in urban areas typically subside after sundown as O_3 reacts with nitric oxide (NO) to form nitrogen dioxide (NO_2), a process known as titration. The O_3 forecast season includes the summertime months (roughly May through September) in most of the United States. However, the O_3 season can be year-round in regions with warmer and drier climates.

From 1978 through 1997, the EPA's O_3 standard was based on the 1-h NAAQS level of 0.12 ppm (or 124 ppb). In 1997, the EPA revised the NAAQS for O_3 to reflect newer research indicating that adverse health effects could occur at lower but prolonged O_3 concentrations. Accordingly, the NAAQS level for the 8-h average O_3 concentration was set to 0.08 ppm (or 84 ppb). The EPA (2004b) estimated that about 160 million Americans are exposed annually to 8-h O_3 concentrations that exceed the new NAAQS, revealing the widespread need for O_3 forecasts. These forecasts are designed to promote awareness of potentially unhealthy air conditions and voluntary behavior modifications (such as limiting outdoor activities and reducing automobile usage) by which individuals and organizations can minimize the risks of

exposure to and minimize anthropogenic contributions to the air quality problems. In general, air quality forecasts are issued for entire metropolitan areas. If the NAAQS are exceeded at a single monitoring site in a metropolitan area, then that metropolitan area is said to be in violation of the NAAQS for that day.

The EPA has a long-standing commitment to public outreach on the subject of air quality and its effects on human health and the environment. To improve the communication of daily air quality information to the public and to use a consistent system nationwide, the EPA revised its AQI in 1997 to include a simple color scheme based on the NAAQS for O₃ and particulate matter (PM). In addition to the adaptation of the new AQI, the EPA coordinates the monitoring and data collection programs for pollutants, and the EPA maintains relationships with state and local agencies that provide and use the data and issue air quality forecasts. Currently, state and local agencies issue daily air quality forecasts for more than 300 cities nationwide (Wayland et al. 2002; R. Wayland, personal communication, 2004), and that number has been steadily increasing. The EPA quality checks, disseminates, and archives the air quality forecast information for public use under the AIRNow program (online at <http://www.epa.gov/airnow>). A national AQF system enables the EPA to substantially advance the air quality guidance it provides to the public.

NOAA is responsible for weather, water, and climate forecasts for the United States, and it develops the advanced understanding needed in atmospheric sciences to improve these forecasts. For decades, NOAA and the EPA (and forerunner agencies) have collaborated in research to improve understanding of air quality. A first major step toward a national air quality forecast capability was NOAA's pilot study of predicting O₃ for the New England Region in 2002 using MAQSIP-RT, MM5-Chem, and HYSPLIT-O₃ (cf. Stockwell et al. 2002). This pilot study provided overall insight into the state-of-the-science and expectations for an operational AQF capability (Kang et al. 2004). A national AQF system links NOAA's real-time weather observations, predictions, and expertise with state-of-the-science photochemical model development.

The AQF system described herein provides numerical guidance (that is, model output) of predicted ground-level concentrations of O₃, thus allowing state and local agencies to use those data in issuing local air quality forecasts. This system was tested with twice-daily runs on the National Centers for Environmental Prediction's (NCEP's) supercomputing system during the summers of 2003 and 2004 (cf. Eder et al. 2003; McQueen et al. 2004). The initial AQF capability was implemented into operations in September 2004 for O₃ predictions for the northeast United States. Within five years (cf. Davidson et al. 2004), the AQF system will be extended to a consolidated national numerical guidance product for multipollutant AQF by expanding to a national domain and testing a predictive capability for particle pollution [i.e., fine PM of diameter less than 2.5 μm (PM_{2.5})].

Currently, the AQF system is based on NCEP's Eta Model (Black 1994; Rogers et al. 1996) and the EPA's Community Multiscale Air Quality (CMAQ) Modeling System (Byun and Ching 1999; Byun and Schere 2005). This AQF system represents the first operational forecast implementation of CMAQ. Section 2 describes some of the scientific and technical issues that were considered for linking the Eta Model with CMAQ. Additional detail is provided to illustrate how the AQF system differs from the regulatory applications of CMAQ (which typically use meteorological fields from MM5), as well as where the CMAQ system was modified for the operational supercomputing environment. Section 3 provides an overview of the components of the AQF system, including details of the grid structure, input emissions data, CMAQ model options, and operational timelines. Section 4 shows some examples of output from the AQF system and interpretation in conjunction with the AQI. Finally, section 5 is a summary and a brief discussion of the future plans for the AQF system.

2. Issues for linking the Eta Model and CMAQ

The AQF system, like other operational systems, is designed to provide numerical guidance products to the users in a timely manner. In linking the Eta Model and CMAQ, a range of options was considered, from a tight coupling on the same coordinate systems and grids to a

looser coupling with interpolation from one coordinate and grid system to another. The choices made here represent those that are likely to produce the best scientific results within NOAA's current resource and operational timing constraints.

a. Coupling the Eta Model with CMAQ

The meteorology input for the national AQF system is based on output from NCEP's Eta Model (also known as the North American Mesoscale, or NAM, model), which is run four times daily for North America at a horizontal grid spacing of 12 km. The operational domain for the Eta Model covers the continent of North America with enough model grid cells to comfortably forecast for the United States, including Alaska, Hawaii, and Puerto Rico. The initial focal area for the AQF system is a small subset of the Eta Model forecast domain. In general, air quality modeling requires a high degree of coupling between the meteorology and photochemical models to maximize the consistency of the mass in the simulation domain and the individual grid cells (Byun 1999b). Several possible paths for coupling CMAQ to the Eta Model were considered.

Ideally, CMAQ should use the same horizontal grid spacing and staggering, the same map projection, and the same vertical coordinate as the meteorological fields from the Eta Model to maintain mass consistency. However, the Arakawa E-grid (Arakawa and Lamb 1977) and the rotated latitude-longitude map projection that are used by the Eta Model are not currently supported by CMAQ, which uses the Arakawa C-grid and a number of other map projections. Converting CMAQ to run on the Arakawa E-grid would have required substantial recoding of the CMAQ transport algorithms and data structures. Also, although CMAQ uses a generalized vertical coordinate to facilitate close coupling with meteorology models (Byun 1999a), the Eta Model's step-mountain vertical coordinate would be especially difficult to replicate in the CMAQ model. Furthermore, the full Eta Model forecast domain is currently too large to be used by CMAQ and still meet the delivery requirements on run-time of approximately two hours. Hence, this ideal solution was not pursued.

Another option for coupling the Eta Model with CMAQ is to use data files that are already disseminated by NCEP. Eta Model output is routinely delivered to operational customers as GRIdded Binary (GRIB) files written for predefined spatial domains at 3-h intervals and typically on pressure surfaces. However, CMAQ requires some fields that are generally unavailable in those GRIB files in order to estimate the volume over which pollutants are dispersed and to estimate dry deposition velocities for photochemical species. In addition, the pressure coordinate in the widely available Eta Model output files is not easily converted to the generalized coordinate system. CMAQ also requires meteorological fields at a minimum of hourly intervals. Thus, using available Eta Model output clearly would not provide close spatial and temporal coupling between the two modeling systems.

As a compromise, coupling between the Eta Model and CMAQ in the AQF system involves horizontal and vertical interpolation of the Eta Model output hourly from 0 to 48 h to a grid structure that is readily ingested by CMAQ. Using a series of postprocessors, the Eta Model output is recast onto a hydrostatic sigma-P vertical coordinate structure and a Lambert conformal map projection of an Arakawa-C staggered horizontal grid that also has 12-km horizontal grid spacing. In addition, NCEP diagnoses additional variables that are necessary for CMAQ from the raw Eta Model output as part of the postprocessing sequence. This approach is advantageous because it does not entail any modifications to the Eta Model or to CMAQ, and it minimally impacts the operational suite at NCEP. To mitigate the effects of horizontal and vertical interpolation used in the Eta Model postprocessing, a robust mass-correction algorithm is implemented in CMAQ to conserve air chemical species (see section 3c).

b. Emissions

In addition to meteorology, CMAQ requires emissions data for various pollutant sources at the appropriate spatial, temporal, and chemical resolutions. Since real-time collection, quality control, and transmission of emissions data from state agencies to the EPA and then to NOAA currently does not exist, real-time emissions forcing is not an option for AQF. As an alternative,

the EPA maintains a historical national emissions inventory (NEI; available online at <http://www.epa.gov/ttn/chief/net/index.html>) with data for mobile sources (e.g., vehicular traffic), stationary area and point sources (e.g., power plants), and natural and agricultural sources (e.g., wild fires and animal operations). The NEI is generally updated triannually, but modifications can be made to project emissions growth or reduction for any area and year, as is typically done for regulatory applications of CMAQ. Some emissions data can be predefined based on the historical emissions patterns, while others must be set using criteria from the specific forecast day. For example, biogenic emissions depend strongly on meteorological factors such as temperature and solar insolation. In addition, mobile source emissions and certain industrial source emissions are strongly influenced by the traditional work week. These factors must be considered on a day-to-day basis to provide input for CMAQ.

c. CMAQ boundary conditions

Since CMAQ is a limited-area model, concentrations of chemical species must be specified at the lateral boundaries to account for mass advected into the computational domain. The absence of real-time chemical observations presents a challenge for the AQF system in determining the lateral boundary conditions for CMAQ. It is particularly difficult since the limited-area forecast domain includes lateral boundaries that intersect large land masses having heterogeneous sources of emissions. Even if the emissions were known perfectly, it is impossible to accurately specify time- and space-dependent chemical boundary conditions *a priori* based on the daily air mass without real-time data. As a compromise, the lateral boundary conditions for O₃ in the AQF system are set using a background continental profile based on climatology that is modified in the upper troposphere to reflect O₃ forecasts from NCEP's Global Forecast System (GFS; Kanamitsu 1989; Caplan et al. 1997). All other chemical fields have time-invariant lateral boundary conditions based on continental profiles, as is typically done for regulatory applications of CMAQ. To the degree that the model is sensitive to lateral boundary conditions, it can sometimes be difficult to simulate high and low concentration episodes well

with (effectively) fixed lateral boundary conditions in the lower troposphere. This effect will diminish when the domain becomes larger such that the eastern and western lateral boundaries will be largely over water and farther removed from the target forecast regions.

d. Computational aspects of CMAQ for AQF

The forecast version of CMAQ (CMAQ-F) is based on the community version of CMAQ (available online at <http://www.cmascenter.org>). Most of the modifications to convert CMAQ to CMAQ-F focused on tailoring the model's performance toward the operational supercomputing hardware and the parallel environment at NCEP and for effectively managing input and output (I/O) processes. In the community version of CMAQ, the Single Program and Multiple Data (SPMD; Flynn 1966) paradigm is used for parallel processing, and the computational domain is decomposed horizontally in space, where each partitioned domain is assigned to a processor. For the output operations, one of the processors is also designated as the output processor. When a processor completes its computations, it sends its data to the output processor, which collects data from all of the worker processors and writes the data to disk in a round-robin fashion. All of the processors are then synchronized at the end of the output process. This design was chosen so that CMAQ could remain modular at the level of the science processing. One major drawback of this parallelization design is the synchronization overhead which increases as the number of processors increases.

A Multiple Instruction and Multiple Data approach (MIMD; Flynn 1966), where writing to disk is overlapped with computation, is used in CMAQ-F. In the AQF system, $m + n$ processors are allocated to run the model where m processors are I/O group processors that are strictly designated for output operations and n processors are workers that perform computation only. The basic parallelization principle is still the same: the computational domain is decomposed horizontally in space, and each of the n processors reads its own portion of data from the input files, computes with its own data, and communicates among those n processors for data exchange purposes. In CMAQ-F, however, when a processor in the worker group

finishes its work at the end of a time step, it sends the output data to the I/O processor group. Once the data transmission is completed, the worker processor resumes computation without any explicit synchronization with other worker processors. The modular structure of the CMAQ code has been somewhat compromised in CMAQ-F so that the science processes that generate output (for example, vertical diffusion and cloud processing) are no longer easily replaceable. However, this design eliminates the synchronization overhead and reduces the overall execution time by overlapping computation with output processing. This design is also scalable, which is attractive for simulating on larger computational domains within an operational timetable by adding more processors. The approach to parallelization in CMAQ-F is similar to that used in the Eta Model.

3. The Eta/CMAQ AQF system

The Eta/CMAQ AQF system provides twice-daily 48-h gridded O₃ predictions as air quality forecast guidance for the United States. The current forecast domain covers the northeast United States with a 12-km horizontal grid spacing on a Lambert Conformal map projection (i.e., new NCEP GRIB map 146). All fully functional photochemical air quality modeling systems, including the Eta/CMAQ AQF system, have three primary components: meteorology, emissions, and chemistry models. These components are discussed below, as are the operational timelines for the AQF system. In addition, a verification component, which is not discussed here, is used to gauge the accuracy of ground-level O₃ predictions.

a. Meteorology

In the current implementation, forecast data from the 60 Eta Model layers on the full horizontal domain are interpolated to 22 hydrostatic sigma-P layers for CMAQ using a modified version of the Eta Model Postprocessor. Many of the 22 layers are in the lower troposphere within the PBL where most of the photochemical activity takes place that is important for surface (and near-surface) O₃ generation. There are approximately 12 layers below 2 km AGL, and the

lowest layer thickness is ~39 m. The geopotential height is interpolated to the 23 layer interfaces using virtual temperature, and that height is used to derive the temperature hydrostatically from thickness so that temperature and height are in hydrostatic balance. As necessary, the Eta Model Postprocessor diagnoses additional forecast variables for the AQF system using the Eta Model's algorithms to maintain a tighter coupling with CMAQ. Of primary importance to the AQF system is the forecast PBL height (or mixing height), which is used in the emissions processing to calculate plume rise and is used in the chemistry transport model to determine the extent of the dilution of primary and secondary pollutants (cf. Dabberdt et al. 2004). In addition, several variables are required to compute dry deposition velocities for chemical species, a key sink process that can affect the accumulation of O₃. The dry deposition velocities are influenced by microscale activity in the vegetation within each grid cell. The suite of new output variables also includes land use category (to define a land-water mask), plant canopy water, canopy conductance, and surface exchange coefficient.

Next, NCEP's Product Generator software is used to extract a subset of the hydrostatic sigma-level data from the Eta Model domain over the CMAQ forecast domain. In addition, the Product Generator places all variables on the unstaggered Arakawa A-grid and writes them in GRIB format. The Product Generator performs either grid-to-grid bilinear interpolations or nearest-neighbor mappings for the fields in the Eta Model Postprocessor output files; no new variables are created in the Product Generator. For most meteorological fields, a standard four-point bilinear interpolation is used to project Eta Model output on the CMAQ forecast domain. Categorical data such as land cover, as well as fields that have strong ties to land cover or a land-water mask, should not be interpolated and are filled directly from the closest Eta Model grid cell to the target CMAQ grid cell. However, use of both bilinear interpolation and nearest-neighbor mapping to project the Eta Model fields onto the CMAQ domain may introduce some mass and physical inconsistencies. For example, the horizontal wind components are computed using bilinear interpolation, but the friction velocity and mixing depth use values from the nearest grid cell as those fields can vary greatly over land and water. In the AQF system, bilinear

interpolation is always used for the 3D state variables, while nearest-neighbor mapping is generally used for surface-related 2D fields.

The final step to prepare the meteorology for input to CMAQ is done through a new preprocessor for CMAQ, called PREMAQ, which is based on algorithms from CMAQ's Meteorology-Chemistry Interface Processor (MCIP; Byun et al. 1999a). The purposes of PREMAQ are to put the Eta Model forecast fields onto the horizontal and vertical structure that CMAQ expects, to create all of the atmospheric state variables that are required in the chemistry transport model, and to perform time-dependent emissions calculations. PREMAQ translates fields from the Arakawa A-grid to the Arakawa C-grid and calculates air density and Jacobian (that is, a time-dependent function of surface pressure, air density, and gravity in the hydrostatic sigma coordinate system), which are used as state variables in the mass-conserving CMAQ general equations. PREMAQ also computes the dry deposition velocities for various photochemical species as required by the chemical mechanism used by the chemistry transport model. Unlike in MCIP, the meteorologically dependent emissions processing is included in PREMAQ to streamline the operational pipeline and minimize I/O requirements.

b. Emissions

The input emission data for the AQF system are based on area, non-road, and point source inventories from the EPA 2001 NEI with some enhancements to better estimate the emissions for the current year. In particular, point source emission estimates include regional adjustments to the NO_x emissions based on projected energy usage, and the 2002 commercial cooking inventory was also included. The 1995 Canadian and 1999 Mexican Big Bend Regional Aerosol and Visibility Observational Study (BRAVO) emission inventories are combined with the 2001 NEI to form the continental data set. The Vehicle Miles Traveled (VMT) data from the 1999 NEI are used in the AQF system as background for the mobile source emission calculations.

The processing of the emissions data for the AQF system has been adapted from the Sparse Matrix Operator Kernel Emissions (SMOKE) modeling system (Houyoux et al. 2000). SMOKE uses sparse-matrix algorithms to efficiently generate emission files required by air quality models such as CMAQ. This approach permits rapid and flexible processing of emissions data, both of which are critical in an operational environment. The processing steps of chemical speciation, temporal allocation, and spatial allocation in SMOKE are separated into independent operations. The results from these steps are merged together at a final stage of processing using vector-matrix mathematics.

For the AQF system, the emissions processing is divided into two components: calculation of emissions fields that are independent of meteorological fields and can be made available *a priori*, and calculation of emissions fields that are dependent on meteorology. The emissions processing that is independent of the meteorological fields is computed outside of the AQF system using the SMOKE model and stored in static files that are used on the appropriate day. The remainder of the emissions processing is integrated into PREMAQ and calculated on an hourly basis in real time. The processing of the major emissions categories is summarized in Table 2.

Emissions from area sources (e.g., agricultural fields, large open mining operations, forests, or aggregates of closely spaced point sources such as residential housing) are assumed to vary in predetermined spatial and temporal patterns that can be calculated in advance for any day of the year. Therefore, area source emissions are calculated from the NEI, adjusted for the current forecast year, and stored as static files for the AQF system.

Emissions from point sources (e.g., industrial stacks) are assumed to have a predetermined temporal variability. However, since point sources are released at different heights in the atmosphere (depending on the height of the stack) usually as a heated gas, a plume rise algorithm is required to calculate the top and bottom heights of the plume. Plume rise is calculated from Eta Model forecasts of vertical and horizontal wind components, air temperature, heat flux, mixing height, and water vapor mixing ratio. Given these, the plume is partitioned into

each of the model layers intersecting the plume based on the pressure in each layer and the stability of the column. Only the plume rise that occurs in the vertical column of cells at the horizontal location of the stack is calculated in PREMAQ; the calculation of plume transport to neighboring model grid cells is done in CMAQ.

Biogenic emissions (e.g., hydrocarbon emissions from vegetation and nitric oxide emissions from soils) are highly dependent on meteorological fields. Therefore, the Biogenic Emissions Inventory System version 3 (BEIS3; Pierce et al. 1998; Pierce et al. 2002) is directly integrated into PREMAQ. The biogenic emissions are calculated using the Eta Model forecasts of solar radiation, surface temperature, surface pressure, and 24-h accumulated rainfall.

Mobile source emissions processing depends on temperature, vehicle activity, and vehicle fleet information. A highly detailed emissions model of on-road sources (MOBILE6) has been developed by the EPA (2003), and it has also been integrated into SMOKE. However, the SMOKE implementation of MOBILE6 is computationally expensive and inefficient for use in the AQF system. Therefore, an efficient method for estimating mobile source emissions based on SMOKE and MOBILE6 has been developed for the AQF system. First, mobile source emissions are computed using SMOKE and MOBILE6 with temperature fields from a previous multimonth time period. Using these data, a relationship between the mobile source emissions and the temperature was obtained using a nonlinear least squares fit of the emission data for each grid cell in the forecast domain, each emitted chemical species, each hour of the day, and each day of the week. This level of detail is necessary because of the complex assumptions built into the MOBILE6 model, especially with respect to vehicle activity, time of day, and day of week. In addition, separate coefficients are calculated for the evaporative and exhaust components of the emission estimates. A quadratic function is used to fit the emission data to the temperature data. The coefficients calculated using the nonlinear least squares fit are saved for each grid cell, each chemical species, each hour of the day, and each day of the week. These coefficients are used with the Eta Model forecast temperature field to calculate the mobile source emissions in the AQF system. Only this final calculation for mobile source emissions is included in

PREMAQ since the coefficients can be determined *a priori*. This calculation is very efficient, and it generates mobile source emission estimates that are highly correlated with using the complete SMOKE and MOBILE6 method. However, this method is not a replacement for MOBILE6 since it depends entirely on the detailed information contained in MOBILE6.

At the conclusion of the PREMAQ processing, emissions from area, point, biogenic, and mobile sources are combined to form a single 3D gridded representation of the emissions for various photochemical species. This emissions file reflects hourly meteorological variations, as well as climatological and seasonal effects.

c. Chemistry

The CMAQ Chemistry Transport Model (CCTM) is used to provide the forecasts of photochemical pollutants in the national AQF system. In the initial AQF capability for O₃ forecast guidance, gas-phase and aqueous chemistry are included; aerosol and heterogeneous chemistry processes, which can be computationally expensive and are less critical for O₃ forecasting, are omitted. The current version of the CCTM in the AQF system uses the Carbon Bond 4 (CB4) chemical mechanism (Gery et al. 1989). This highly compact chemical mechanism reduces the complexity of the organic chemistry by employing a structural lumping technique that groups organic compounds according to bond type. The CB4 mechanism has proven to be very successful in simulating ambient O₃ concentrations and is widely used for regional photochemical modeling (cf. Russell and Dennis 2000). Although the Eta Model's top is at 25 hPa to represent lower-stratospheric dynamics, CMAQ's model top is 100 hPa because stratospheric O₃ changes rather slowly under normal circumstances.

Chemical advection is operator-split into each of three spatial dimensions and computed using contravariant wind components (i.e., weighted by the inverse of the map-scale factors squared; see Byun et al. 1999b). Errors created by dimension splitting are corrected by density weighting before and after each 1D advection step. The numerical advection scheme is the piecewise parabolic method (Colella and Woodward 1984), which is an efficient monotonic

scheme with minimal numerical diffusion. This is particularly important for photochemical transport modeling since pollutant distributions are spatially heterogeneous and characterized by sharp gradients in source regions. Vertical advection is always computed after the horizontal advection operations to allow for diagnosis of vertical wind components that satisfy the mass continuity equation. A robust mass correction algorithm is implemented in CMAQ in the AQF system to ensure conservation of air chemical species (R. Yamartino, personal communication, 2002).

CMAQ uses a semiimplicit eddy diffusion scheme based on bulk PBL scaling within the PBL and local shear and stability above the PBL (Byun et al. 1999b). Cloud processes include aqueous chemistry, subgrid convective vertical transport, and wet scavenging and deposition. CMAQ's cloud module is based on the Regional Acid Deposition Model (Chang et al. 1987) with updated chemical and physical parameters (Roselle and Binkowski 1999). Convective and nonconvective clouds are diagnosed from the Eta Model forecasts of convective and nonconvective precipitation along with forecast temperature and humidity profiles. The photolysis rates in CMAQ are calculated using the approach described by Madronich (1987). Cloud effects on photolysis are based on cloud cover diagnosed from Eta Model forecasts of relative humidity. Diagnosed cloud fraction, base, top, and average liquid water content are used to modify clear-sky photolysis rates that are computed *a priori* using a delta-Eddington two-stream radiative transfer model (Joseph et al. 1976; Toon et al. 1989).

Chemical dry deposition velocities are computed in PREMAQ using an electrical resistance analog model (Pleim et al. 2001). Atmospheric and boundary layer resistances are based on atmospheric surface layer parameters from the Eta Model (e.g., friction velocity and surface heat exchange coefficient). Canopy resistance is a parallel combination of surface resistances (leaf cuticle and ground) and stomatal resistance. The bulk stomatal resistance is derived from the moisture canopy conductance from the Eta Model. Surface resistances are scaled by solubility and chemical reactivity of each chemical species. Several surface parameters from the Eta Model (e.g., leaf area index, fractional vegetation coverage, canopy

water content, and roughness length) are also used in the surface resistance calculations. These surface parameters often have strong ties to the land use (or vegetation type) database that is used in the Eta Model.

d. Operational timelines

The AQF system is given an operational time window of two hours to complete preprocessing, the CMAQ model forecast, and all postprocessing. The photochemical initial conditions for CMAQ are set from the previous forecast cycle. Lateral boundary condition profiles were discussed in section 2c. In the current implementation, the CMAQ simulation uses 1 I/O and 32 computational processors. The output files from CMAQ are processed (without interpolation) into GRIB format for dissemination.

Figure 2 illustrates the forecast cycle for the AQF system, which generates 48-h forecasts using the Eta Model's 0600 UTC and 1200 UTC cycles. The primary CMAQ forecast for next-day surface-layer O₃ is based on the current day's 1200 UTC Eta Model cycle. Forecast products from the 1200 UTC cycle are available daily no later than 1330 eastern daylight time (EDT) so they can be used by air quality forecasters who typically issue next-day forecasts by mid-afternoon. The target forecast period is local midnight through local midnight for northeast United States (e.g., 0400 UTC to 0400 UTC). An additional 8 h are required beyond midnight to calculate 8-h average O₃ concentrations used to assess the NAAQS and to compute the AQI. In addition to the primary forecast, a daily early-morning update to the previous day's forecast is issued no later than 0900 EDT based on the current day's 0600 UTC cycle. The forecast update is targeted for the 22-h period from 0600 UTC through 0400 UTC (0200 EDT on the current day through 0000 EDT on the following day).

4. Forecasting O₃ for the northeast United States

The AQF system was run twice daily at the NWS/NCEP for preoperational evaluation to support the summer 2003 and 2004 O₃ forecast seasons for the northeast United States. The

output files included gridded 1-h and 8-h average surface O₃ concentrations for comparisons against the NAAQS. Products from the 2003 and 2004 O₃ forecast seasons were provided to a limited focus group of experienced air quality forecasters who evaluated the utility of the AQF system and provided feedback for development and refinement of the system. In addition, the AQF system products were made publicly available by NOAA (online at <http://weather.gov/aq>) as experimental guidance during the 2004 O₃ forecast season.

To achieve full operational status (cf. Davidson et al. 2004), the AQF system met performance standards for accuracy ($\geq 90\%$ exceedances and nonexceedances forecast correctly) and product availability ($\geq 95\%$ ontime delivery of guidance), as defined by NOAA, for the 2003 and 2004 O₃ forecast seasons. Kang et al. (2004) describe additional verification protocols (that is, statistical measures) that have also been used to evaluate the performance of the AQF system. Eder et al. (2003) and Ryan et al. (2004) provide preliminary discussions of the performance of the AQF system; thus statistical verification of the AQF system will not be discussed here. Additional rigorous evaluation of the air quality forecasts (including an expanded suite of statistical measures and subjective evaluation of 3D fields from the Eta Model and CMAQ) was also performed during both the 2003 and 2004 O₃ forecast seasons by development groups from both NOAA and the EPA.

The 2003 and 2004 O₃ forecast seasons had anomalously few days with O₃ exceedances in the northeast United States, in part, because of the predominant cooler and wetter than normal conditions (EPA 2004a). Figures 3–8 show a sample of the meteorology and O₃ observations and predictions from the AQF system with a focus on 22 July 2004, one of the few days with measured high O₃ concentrations in the northeast United States in 2004. The forecasts shown are initialized at 1200 UTC 21 July 2004 to provide numerical guidance for the target forecast day (see Fig. 2) of 22 July 2004. On 22 July 2004, a cold front associated with a low pressure system centered east of Hudson Bay (not shown) was sweeping slowly across the Great Lakes and the Ohio Valley, bringing Canadian air into the northwestern part of the forecast domain. The eastern United States was dominated by southerly and southwesterly flow and a weak surface

pressure gradient in advance of the cold front. High pressure systems were centered along the Gulf Coast and in the Atlantic Ocean east of the Canadian Maritime provinces. At 1200 UTC, a weak upper-level ridge extended just west of and along the Appalachian Mountains (not shown), which, in conjunction with light winds, clear skies, and weak vertical motion, is favorable for summertime surface O₃ formation in the northeast United States east of the upper-level ridge (Ryan et al. 2000). Observed maximum temperatures (not shown) were greater than 32°C (~90°F) throughout the Gulf Coast states, South Carolina, western Tennessee, western Kentucky, and southern Illinois. Observed maximum temperatures were greater than 26°C (~80°F) throughout the remainder of the forecast domain ahead of the cold front, and they were generally 21–26°C (~70–80°F) behind the cold front.

Figure 3 presents the 1-h average surface O₃ forecast guidance from the AQF system valid at 2000 UTC 22 July 2004 (4 p.m. EDT, or approximately when the peak hourly O₃ concentration is observed) compared with surface O₃ observations from the EPA's Air Quality System [AQS, formerly known as the Aerometric Information Retrieval System (AIRS)]. In Fig. 3, the highest observed concentrations of O₃ (greater than 90 ppb) are near Atlanta, Georgia; Charlotte, North Carolina; and Harrisburg, Pennsylvania; throughout New Jersey, eastern Pennsylvania, and southeastern New York; and along an axis from New York City through New England to Portland, Maine. The AQF system forecasted these moderately high values well in the next-day (32-h) forecast shown in Fig. 3. In addition, somewhat elevated values of O₃ were also well-predicted in the mid-Atlantic region from North Carolina to Delaware, and near Knoxville, Tennessee; St. Louis, Missouri; and Birmingham, Alabama. The AQF system overpredicted the O₃ concentrations near Chicago, Illinois on that day, which may be, in part, related to the overprediction of the near-surface air temperature by the Eta Model (refer to Fig. 4). High concentrations of O₃ were forecast over southern Lake Erie and the southern Chesapeake Bay. These concentrations cannot be verified since there are no stationary O₃ monitors there, but the predictions are likely linked to low PBL heights over water (see Fig. 5)

which provide a shallow vertical column to contain and mix pollutants transported from nearby land-based emission sources.

Figure 3 also shows that low concentrations of O₃ were both forecast and observed at 2000 UTC ahead of the cold front near Evansville, Indiana; Cincinnati, Ohio; Charleston, West Virginia; Pittsburgh, Pennsylvania; and Buffalo, New York. These low concentrations at 2000 UTC can be attributed, in part, to the well-forecast convection ahead of the cold front as seen in the visible satellite image in Fig. 6. The Eta Model forecast the timing and placement of the convection well, as can be inferred from the spatial patterns in the reduction of near-surface air temperature in that region (Fig. 4), the collapse of the PBL (Fig. 5), and the forecast convective precipitation (not shown). Convective activity often serves as a sink of O₃ in the lower troposphere due to the redistribution of pollutants by vertical mixing in a deep column. Additionally, the presence of clouds results in the attenuation of downward shortwave radiation and consequently lower photolysis rates, which, in turn, limit the formation of O₃ in the presence of cloud cover. Low O₃ concentrations were also both forecast and observed (Fig. 3) in areas of Wisconsin and Michigan that were behind the cold front. These low O₃ concentrations are linked to the cleaner and cooler air mass behind the front. Figures 3–6 suggest that the AQF system can generate useful one-day hourly O₃ forecast guidance for cities throughout the northeast United States. Figure 3 shows that the spatial extent and magnitude of the O₃ concentrations can be well forecast by the AQF system, even in the presence of relatively complex warm-season meteorology.

Figures 3–6 also illustrate many aspects of the well-documented strong influences that the quality of the meteorological simulations have on the chemistry model simulations. Forecast meteorological fields for most state variables, as well as precipitation and PBL height, are directly input to the chemistry model, so errors in the meteorology simulation will often be reflected as errors in the chemistry model forecast. Therefore, it should be emphasized that the uncertainties in the meteorological model forecast guidance must be considered in conjunction with O₃ concentration forecast guidance from the AQF system when issuing AQI forecasts. For

example, the overprediction of near-surface air temperature in the Eta Model near Chicago (Fig. 4), combined with forecast low-level convergence, created conditions that were conducive to O₃ formation in CMAQ. However, cloudy conditions were observed in that region (Fig. 6) which were not captured by the Eta Model, as can be inferred from the forecast deep PBL (Fig. 5) and downward shortwave radiation at the surface (not shown). Thus the observed near-surface air temperatures (discussed above) and surface O₃ concentrations (Fig. 3) were somewhat lower than forecast by the AQF system. In addition, Fig. 3 shows the forecast plumes of high O₃ concentrations extending to the southeast of Atlanta and Birmingham following the forecast northwesterly low-level wind trajectory (Fig. 4). Although neither of these plumes can be verified because there are no O₃ monitors in the forecast plumes, errors in forecast wind speed and direction could contribute to a forecast error in the downwind location of the transported O₃ plumes in the AQF system. Similarly, if the onshore flow from a sea breeze penetrates too far inland in the Eta Model forecast, it could contribute to underforecast O₃ concentrations due to the erroneous influx of clean maritime air. These examples illustrate some of the challenges of forecasting the complex interplay among the atmospheric dynamics, thermodynamics, and chemistry, each of which contributes to the guidance generated by the AQF system.

By contrast, the well forecast timing and placement of the surface cold front by the Eta Model (see Figs. 4 and 5) contributed to defining well the spatial extent of the elevated O₃ concentrations forecast by CMAQ in the AQF system. If the timing of the surface cold front had been too slow to allow near-surface air temperatures and PBL heights to continue to rise in the mid-afternoon along the Ohio River Valley, where large emission sources of O₃ precursors are located, the AQF system may have erroneously forecast elevated O₃ concentrations. Likewise, if the cold front was forecast to advance too quickly, the peak O₃ concentrations could have been underforecast east of the Appalachian Mountains from the effects of ill-timed convection. Furthermore, the Eta Model forecast well the clear and warm conditions and the southerly flow in Pennsylvania and New Jersey, and into New England that resulted in a good forecast for high O₃ concentrations along the Delaware and Hudson River Valleys and north of Boston. In

particular, correctly predicted low-level convergence in the Eta Model (Fig. 4) resulted in correctly forecast locally high O₃ concentrations near Allentown, Pennsylvania, and in southeastern New Hampshire (Fig. 3).

Figure 7 presents a time series comparison of forecast and observed hourly O₃ concentrations at Tucker, Georgia (approximately 20 km northeast of Atlanta). Figure 7 illustrates the diurnal cycle of the near-surface urban O₃ concentrations, and it shows that the AQF system captured that cycle well. The peak hourly O₃ concentrations are ~10 ppb in error, which is in range of typical performance for the AQF system [mean monthly bias of ~8-12 ppb for the summer of 2004 (D. Kang, personal communication, 2004)]. The AQF system correctly forecast the trend toward improving air quality conditions on the second day (or the target forecast period; see Fig. 2), and shows more skill than a persistence-based forecast. Using the data shown in Fig. 7, the maximum 8-h average O₃ concentration forecast by the AQF system on the first day was 120 ppb, which is equivalent to an AQI value of 190, or a code red for unhealthy air quality conditions. [See Table 1 and EPA (1999b) for details of the O₃ concentration-to-AQI conversion.] The observations indicate that the AQF system forecast verified well for AQI, as the observed maximum 8-h average O₃ concentration was 112 ppb, which converts to an AQI value of 169, which is also a code red. Similarly, on the second day of the forecast shown in Fig. 7, the AQF system forecast a maximum 8-h average O₃ concentration of 86 ppb (AQI value of 104), which is a code orange that indicates unhealthy air quality conditions for sensitive groups. Again, the AQF system verified well as the observed maximum 8-h average O₃ concentration at that AQS monitor was 91 ppb (AQI value of 119), which is also a code orange. Figure 7 suggests that the AQF system can perform well in times when air quality alerts are needed.

Figure 8 presents comparisons of the spatial distributions of the observed and forecast maximum 8-h average O₃ concentrations over the northeast United States for 22 July 2004. Figure 8 shows that the AQF system forecast well the unhealthy air quality conditions due to O₃ (i.e., AQI greater than 100, or at least code orange) near Atlanta; Charlotte; Allentown; northern

New Jersey; eastern New York, including Albany; Hartford, Connecticut; Springfield, Massachusetts; and southern New Hampshire. The AQF system forecast code red conditions southeast of Atlanta that could not be verified because there are no monitoring sites in that forecast area; however, the orientation of the O₃ plume would reflect any errors in the wind direction forecast. A code red was observed near Allentown, but the observed maximum 8-h concentration was 105 ppb, which is on the dividing line between codes red and orange. Figure 8 also shows that the AQF system forecast reasonably well the moderate air quality conditions (code yellow) throughout central North Carolina and parts of South Carolina; near Knoxville, Nashville, and Memphis, Tennessee; and in Birmingham; St. Louis; Indianapolis; Cleveland, Ohio; and Richmond, Virginia. The AQF system captured the dividing line between the good air quality conditions (code green) and widespread moderate conditions east of the Appalachian Mountains. In addition, the good air quality conditions were correctly forecast along Lake Michigan and in Detroit, Michigan. Some slight overpredictions were observed north of Baltimore, Maryland, into southern Pennsylvania, and near the Virginia Tidewater region. Overall, the AQF system correctly forecast the air quality conditions for metropolitan areas throughout the forecast domain, as well as the spatial extent of the widespread moderate and unhealthy air quality conditions in the northeast United States on that day. Figure 8 helps to illustrate further that the AQF system can be a valuable tool for forecasting unhealthy air quality conditions that can be attributed to 8-h average O₃ concentrations in this region.

5. Summary and Future Plans

A national AQF system has been developed by NOAA and the EPA. This AQF system, which became operational in September 2004, is currently based on NCEP's 12-km Eta Model and the EPA's CMAQ modeling system. The initial operational implementation generates next-day numerical forecast guidance for ground-level O₃ for the northeast United States that can be used by the state and local agencies that issue air quality forecasts. The twice-daily

preoperational forecasts during the 2003 and 2004 O₃ forecast seasons demonstrated that the AQF system can be a valuable tool in the air quality forecast process.

As with all operational systems, the AQF system will evolve with time. First, it will be expanded beyond the northeast United States to provide a nationwide AQF capability within five years. The horizontal grid spacing may decrease as computational capacity increases and in conjunction with changes to the Eta Model and successor mesoscale models. There are also plans to expand the AQF system to provide multipollutant forecasts (specifically PM_{2.5}) and to extend the forecast period to two days and beyond. Developmental testing of the AQF system with a detailed representation of aerosol dynamics and chemistry is already underway. In addition, updated emissions data can be incorporated into the AQF system when the logistics of providing near-real-time emissions data from state agencies to the EPA and then to NOAA are improved. PREMAQ may also be parallelized or subsumed into the CMAQ processing as part of future software optimization.

Scientific refinements to the AQF system will continue based on the 2003 and 2004 preoperational evaluations. In addition to the ability to forecast well the harmful concentrations of O₃, the AQF system forecasts good (or code green) conditions well, but the magnitudes of the O₃ concentrations during cloudy periods are often in error. Therefore, a focus on improving cloud and radiation processes in the AQF system, including a tighter coupling between the meteorology and chemistry models, is planned. Effects from wildfires are not included in the current implementation of the emissions but are planned for the PM forecasting applications. When the Weather Research and Forecast Model (WRF) becomes the NAM model at NCEP, it will then provide the meteorology input for the AQF system. A revision of CMAQ to use the WRF map projection, and horizontal and vertical grid structures is also planned in order to reduce the number of interpolations needed in the model linkage and to facilitate a tighter model coupling. Finally, the benefits of a fully coupled system with two-way feedbacks between meteorology and chemistry (i.e., an “online” system; cf. Grell et al. 2004) are being investigated as a means to improve future operational capabilities.

Acknowledgments. The authors are grateful to Eric Rogers for providing initial output data from the Eta Model to build the linkage with CMAQ. The authors also acknowledge Daiwen Kang for processing the ozone observations. The research presented here was performed, in part, under the Memorandum of Understanding between the U.S. Environmental Protection Agency (EPA) and the U.S. Department of Commerce's National Oceanic and Atmospheric Administration (NOAA) and under agreement number DW13921548. Although it has been reviewed by EPA and NOAA and approved for publication, it does not necessarily reflect their views or policies. The authors thank Brian Eder, Thomas Pierce, S. T. Rao, and James Meagher for their technical reviews of this manuscript.

References

- Arakawa, A., and V. Lamb, 1977: Computational design of the basic dynamical processes of the UCLA general circulation model. *Methods in Comput. Phys.*, **17**, 173–265.
- Black, T., 1994: The new NMC mesoscale Eta Model: Description and forecast examples. *Wea. Forecasting*, **9**, 265–278.
- Byun, D. W., 1999a: Dynamically consistent formulations in meteorological and air quality models for multiscale atmospheric studies. Part I: Governing equations in a generalized coordinate system. *J. Atmos. Sci.*, **56**, 3789–3807.
- _____, 1999b: Dynamically consistent formulations in meteorological and air quality models for multiscale atmospheric studies. Part II: Mass conservation issues. *J. Atmos. Sci.*, **56**, 3808–3820.
- _____, and J. K. S. Ching, Eds., 1999: Science algorithms of the EPA Models-3 Community Multiscale Air Quality (CMAQ) Modeling System. EPA-600/R-99/030, Office of Research and Development, U.S. Environmental Protection Agency, Washington, D.C., 727 pp. [Available from U.S. EPA, ORD, Washington, D.C. 20460.]
- _____, and K. L. Schere, 2005: Description of the Models-3 Community Multiscale Air Quality (CMAQ) Model: System overview, governing equations, and science algorithms. *Appl. Mech. Rev.*, in press.
- _____, J. E. Pleim, R. T. Tang, and A. Bourgeois, 1999a: Meteorology-Chemistry Interface Processor (MCIP) for Models-3 Community Multiscale Air Quality (CMAQ) Modeling System. *Science Algorithms of the EPA Models-3 Community Multiscale Air Quality (CMAQ) Modeling System*, D. W. Byun and J. K. S. Ching, Eds., EPA-600/R-99/030, Office of Research and Development, U.S. Environmental Protection Agency, Washington, D.C., 12-1–12-91. [Available from U.S. EPA, ORD, Washington, D.C. 20460.]

- _____, J. Young, J. Pleim, M. T. Odman, and K. Alapaty, 1999b: Numerical transport algorithms for the Community Multiscale Air Quality (CMAQ) chemical transport model in generalized coordinates. *Science Algorithms of the EPA Models-3 Community Multiscale Air Quality (CMAQ) Modeling System*, D. W. Byun and J. K. S. Ching, Eds., EPA-600/R-99/030, Office of Research and Development, U.S. Environmental Protection Agency, Washington, D.C., 7-1-7-56. [Available from U.S. EPA, ORD, Washington, D.C. 20460.]
- Caplan, P., J. Derber, W. Gemmill, S.-Y. Hong, H.-L. Pan, and D. Parrish, 1997: Changes to the 1995 NCEP operational Medium-Range Forecast Model analysis-forecast system. *Wea. Forecasting*, **12**, 581–594.
- Chang, J. S., R. A. Brost, I. S. A. Isaksen, S. Madronich, P. Middleton, W. R. Stockwell, and C. J. Walcek, 1987: A three-dimensional Eulerian acid deposition model: Physical concepts and formulation. *J. Geophys. Res.*, **92**, 14 681–14 700.
- Colella, P., and P. R. Woodward, 1984: The piecewise parabolic method (PPM) for gas-dynamical simulations. *J. Comput. Phys.*, **54**, 174–201.
- Cope, M. E., and Coauthors, 2004: The Australian Air Quality Forecasting System. Part I: Project description and early outcomes. *J. Appl. Meteor.*, **43**, 649–662.
- Dabberdt, W. F., and Coauthors, 2004: Meteorological research needs for improved air quality forecasting: Report of the 11th Prospectus Development Team of the U.S. Weather Research Program. *Bull. Amer. Meteor. Soc.*, **85**, 563–586.
- Davidson, P. M., N. Seaman, K. Schere, R. A. Wayland, J. L. Hayes, and K. F. Carey, 2004: National air quality forecasting capability: First steps toward implementation. Preprints, *Sixth Conf. on Atmos. Chem.*, Seattle, WA, Amer. Meteor. Soc., CD-ROM, J2.10.
- Eder, B., D. Kang, and R. Gilliam, 2003: An evaluation of the Eta-CMAQ air quality forecast model as part of NOAA's national program. Preprints, *Second Annual Models-3 Users Workshop*, Research Triangle Park, NC, Community Modeling and Analysis System

- Center, CD-ROM, 4.5. [Available from CMAS, c/o Carolina Environmental Program, Bank of America Plaza, CB #6116, 137 E. Franklin St., Chapel Hill, NC 27599.]
- EPA, 1999a: Guideline for developing an ozone forecasting program. EPA-454/R-99-009, Office of Air Quality Planning and Standards, Research Triangle Park, NC, 88 pp. [Available from U.S. EPA OAQPS, Research Triangle Park, NC 27711.]
- _____, 1999b: Guideline for reporting of daily air quality – air quality index (AQI). EPA-454/R-99-010, Office of Air Quality Planning and Standards, Research Triangle Park, NC, 29 pp. [Available from U.S. EPA, OAQPS, Research Triangle Park, NC 27711, and available online at <http://www.epa.gov/ttn/oarpg/t1/memoranda/rg701.pdf>.]
- _____, 2003: User's guide to MOBILE6.1 and MOBILE6.2 (Mobile Source Emission Factor Model). EPA420-R-03-010, Office of Transportation and Air Quality, Ann Arbor, MI, 262 pp. [Available online at <http://www.epa.gov/otaq/m6.htm>.]
- _____, cited 2004a: 2004 summer ozone season – national recap. [Available online at <http://www.epa.gov/airnow/2004/ozone-recap/o3-season-end-2004.html>.]
- _____, cited 2004b: 8-hour ozone non-attainment areas. [Available online at <http://www.epa.gov/oar/oaqps/greenbk/gntc.html>.]
- Flatoy, F., O. Hov, and H. Schlager, 2000: Chemical forecasts used for measurement flight planning during POLINAT 2. *Geophys. Res. Lett.*, **27**, 951-954.
- Flynn, M. J., 1966: Very high-speed computers. *Proc. IEEE*, **54**, 1901–1909.
- Gery, M. W., G. Z. Whitten, J. P. Killus, and M. C. Dodge, 1989: A photochemical kinetics mechanism for urban and regional scale computer modeling. *J. Geophys. Res.*, **94**, 12 925–12 956.
- Grell, G. A., J. Dudhia, and D. R. Stauffer, 1994: A description of the Fifth-Generation Penn State/NCAR Mesoscale Model (MM5). NCAR Tech. Note, NCAR/TN-398+STR, National Center for Atmospheric Research, Boulder, CO, 138 pp. [Available from NCAR, P. O. Box 3000, Boulder, CO 80307.]

- _____, S. Emeis, W. R. Stockwell, T. Schoenemeyer, R. Forkel, J. Michalakes, R. Knoche, and W. Seidl, 2000: Application of a multiscale, coupled MM5/chemistry model to the complex terrain of the VOLTAP valley campaign. *Atmos. Environ.*, **34**, 1435–1453.
- _____, S. E. Peckham, R. Schmitz, and S. McKeen, 2004: Fully coupled “online” chemistry within the WRF Model. Preprints, *20th Conf. on Weather Analysis and Forecasting/16th Conf. on Numerical Weather Prediction*, Seattle, WA, Amer. Meteor. Soc., CD-ROM, 12.6.
- Houyoux, M. R., J. M. Vukovich, C. J. Coats, Jr., N. M. Wheeler, and P. S. Kasibhatla, 2000: Emission inventory development and processing for the Seasonal Model for Regional Air Quality (SMRAQ) project. *J. Geophys. Res.*, **105**, 9079–9090.
- Joseph, J. H., W. J. Wiscombe, and J. A. Weinman, 1976: The delta-Eddington approximation for radiative flux transfer. *J. Atmos. Sci.*, **33**, 2452–2459.
- Kanamitsu, M., 1989: Description of the NMC Global Data Assimilation and Forecast System. *Wea. Forecasting*, **4**, 335–342.
- Kang, D., B. K. Eder, A. F. Stein, G. A. Grell, S. E. Peckham, and J. McHenry, 2004: The New England Air Quality Forecasting Pilot Program: Development of an evaluation protocol and performance benchmark. *J. Air and Waste Manag. Assoc.*, in press.
- Lawrence, M. G., and Coauthors, 2003: Global chemical weather forecasts for field campaign planning: Predictions and observations of large-scale features during MINOS, CONTRACE, and INDOEX. *Atmos. Chem. Phys.*, **3**, 267–289.
- Madronich, S., 1987: Photodissociation in the atmosphere. 1. Actinic flux and the effects of ground reflections and clouds. *J. Geophys. Res.*, **92 (D8)**, 9740–9752.
- McHenry, J. N., N. Seaman, C. Coats, A. Lario-Gibbs, J. Vukovich, N. Wheeler, and E. Hayes, 1999: Real-time nested mesoscale forecasts of lower tropospheric ozone using a highly optimized coupled model numerical prediction system. Preprints, *Symp. on Interdisciplinary Issues in Atmos. Chem.*, Dallas, TX, Amer. Meteor. Soc., 125–128.

- _____, W. F. Ryan, N. L. Seaman, C. J. Coats, Jr., J. Pudykiewicz, S. Arunachalam, and J. M. Vukovich, 2004: A real-time Eulerian photochemical model forecast system: Overview and initial ozone forecast performance in the Northeast U.S. corridor. *Bull. Amer. Meteor. Soc.*, **85**, 525–548.
- McQueen, J., and Coauthors, 2004: Development and evaluation of the NOAA/EPA prototype air quality model prediction system. Preprints, *Sixth Conf. on Atmos. Chem.*, Seattle, WA, Amer. Meteor. Soc., CD-ROM, J2.16.
- Pierce, T., C. Geron, L. Bender, R. Dennis, G. Tonnesen, and A. Guenther, 1998: Influence of increased isoprene emissions on regional ozone modeling. *J. Geophys. Res.*, **103**, 25 611–25 629.
- _____, _____, G. Pouliot, E. Kinnee, and J. Vukovich, 2002: Integration of the Biogenic Emissions Inventory System (BEIS3) into the Community Multiscale Air Quality Modeling System. Preprints, *12th Joint Conf. on the Appl. of Air Pollut. Meteor. with the A&WMA*, Norfolk, VA, Amer. Meteor. Soc., J85–J86.
- Pleim, J. E., A. Xiu, P. L. Finkelstein, and T. L. Otte, 2001: A coupled land-surface and dry deposition model and comparison to field measurements of surface heat, moisture, and ozone fluxes. *Water Air Soil Pollut.*, **1**, 243–252.
- Rogers, E., T. L. Black, D. G. Deaven, G. J. DiMego, Q. Zhao, M. Baldwin, N. W. Junker, and Y. Lin, 1996: Changes to the operational “early” Eta Analysis/Forecast System at the National Centers for Environmental Prediction. *Wea. Forecasting*, **11**, 391–413.
- Roselle, S. J., and F. S. Binkowski, 1999: Cloud dynamics and chemistry. *Science Algorithms of the EPA Models-3 Community Multiscale Air Quality (CMAQ) Modeling System*, D. W. Byun and J. K. S. Ching, Eds., EPA-600/R-99/030, Office of Research and Development, U.S. Environmental Protection Agency, Washington, D.C., 14-1–14-8. [Available from U.S. EPA, ORD, Washington, D.C. 20460.]
- Russell, A., and R. Dennis, 2000: NARSTO critical review of photochemical models and modeling. *Atmos. Environ.*, **34**, 2283–2324.

- Ryan, W. F., C. A. Petty, and E. D. Luebehusen, 2000: Air quality forecasts in the mid-Atlantic region: Current practice and benchmark skill. *Wea. Forecasting*, **15**, 46-60.
- _____, P. Davidson, P. Stokols, and K. Carey, 2004: Evaluation of the National Air Quality Forecasting System (NAQFS): Summary of the air quality forecasters focus group workshop. Preprints, *Sixth Conf. on Atmos. Chem.*, Seattle, WA, Amer. Meteor. Soc., CD-ROM, J2.13.
- Stein, A. F., D. Lamb, and R. R. Draxler, 2000: Incorporation of detailed chemistry into a three-dimensional Lagrangian-Eulerian hybrid model: Application to regional tropospheric ozone. *Atmos. Environ.*, **34**, 4361–4372.
- Stockwell, W. R., R. S. Artz, J. F. Meagher, R. A. Petersen, K. L. Schere, G. A. Grell, S. E. Peckham, A. F. Stein, R. V. Pierce, J. M. O’Sullivan, and P.-Y. Whung, 2002: The scientific basis of NOAA’s Air Quality Forecast Program. *Environ. Manage.*, **December**, 20–27.
- Toon, O. B., C. P. McKay, and T. P. Ackerman, 1989: Rapid calculation of radiative heating rates and photodissociation rates in inhomogeneous multiple scattering atmospheres. *J. Geophys. Res.*, **94**, 16 287–16 301.
- Uno, I., and Coauthors, 2003: Regional chemical weather forecasting system CFORS: Model descriptions and analysis of surface observations at Japanese island stations during the ACE-Asia experiment. *J. Geophys. Res.*, **108 (D23)**, 8668, doi:10.1029/2002JD002845.
- Vaughn, J., and Coauthors, 2004: A numerical daily air quality forecast system for the Pacific Northwest. *Bull. Amer. Meteor. Soc.*, **85**, 549–561.
- Wayland, R. A., J. E. White, P. G. Dickerson, and T. S. Dye, 2002: Communicating real-time and forecasted air quality to the public. *Environ. Manage.*, **December**, 28–36.
- Wolff, G. T., and P. J. Liroy, 1978: An empirical model for forecasting maximum daily ozone levels in the northeastern United States. *J. Air Pollut. Control Assoc.*, **28**, 1034–1038.

Figure Captions

- Figure 1. Roles of NOAA, the EPA, and state and local agencies in the development and execution of the air quality forecast system.
- Figure 2. Operational 48-h forecast periods for the AQF system. Simulations are initialized at 0600 UTC and 1200 UTC daily. Gray bars indicate the target air quality forecast period of local midnight to local midnight, eastern daylight time.
- Figure 3. Forecast 1-h average surface O₃ concentration (in ppb) from the AQF system compared with observations, valid 2000 UTC 22 July 2004. The forecast was initialized at 1200 UTC 21 July 2004. The O₃ observations are overlaid in diamonds using the same color scale as the AQF system forecast. The color scale does not align with the AQI.
- Figure 4. Forecast 2-m air temperature with near-surface wind vectors from the Eta Model, valid at 2000 UTC 22 July 2004. The forecast was initialized at 1200 UTC 21 July 2004.
- Figure 5. Forecast PBL height from the Eta Model, valid at 2000 UTC 22 July 2004. The forecast was initialized at 1200 UTC 21 July 2004.
- Figure 6. Cropped image from the eastern Geostationary Operational Environmental Satellite (GOES-East, which is currently GOES-12). The image is valid at 2000 UTC 22 July 2004. Original image is taken from the online archive maintained by San Francisco State University.

Figure 7. Forecast surface hourly O₃ concentrations (in ppb) from the AQF system compared with observations from AQS monitor 130893001 at Tucker, GA, northeast of Atlanta. The forecast was initialized at 1200 UTC 21 July 2004. The AQF system forecast is shown in squares connected with a solid line. Observations are shown in open circles connected with a dotted line. The target forecast period (0400 UTC 22 July 2004 through 0400 UTC 23 July 2004, refer to Fig. 2) is in white, while the other forecast times are shown in gray.

Figure 8. Forecast surface maximum 8-h average O₃ concentrations (in ppb) from the AQF system compared with observations, valid 22 July 2004. The forecast was initialized at 1200 UTC 21 July 2004, and the graphic represents the target forecast period (0400 UTC 22 July 2004 through 0400 UTC 23 July 2004, refer to Fig. 2). The observed maximum 8-h average O₃ concentrations are overlaid in diamonds using the same color scale as the AQF system forecast. The color scale aligns with the AQI categories for this pollutant.

Table Captions

Table 1. Converting O₃ to AQI. Adapted from EPA (1999b) and <http://www.epa.gov/airnow>.

The AQI conversions for the other criteria pollutants are in EPA (1999b).

Table 2. Summary of emissions processing in the AQF system.

Table 1. Converting O₃ to AQI. Adapted from EPA (1999b) and <http://www.epa.gov/airnow>.

The AQI conversions for the other criteria pollutants are in EPA (1999b).

Max 8-h O ₃ (ppm)	Max 1-h O ₃ (ppm)	AQI	Level of Health Concern	Color Code	Meaning
0.000- 0.064	(a)	0 – 50	Good	Green	Air quality is considered satisfactory, and air pollution poses little or no risk.
0.065- 0.084	(a)	51 – 100	Moderate	Yellow	Air quality is acceptable; however, for some pollutants there may be a moderate health concern for a very small number of people who are unusually sensitive to air pollution.
0.085- 0.104	0.125- 0.164	101 – 150	Unhealthy for Sensitive Groups	Orange	Members of sensitive groups may experience health effects. The general public is not likely to be affected.
0.105- 0.124	0.165- 0.204	151 – 200	Unhealthy	Red	Everyone may begin to experience health effects; member of sensitive groups may experience more serious health effects
0.125- 0.374	0.205- 0.404	201 – 300	Very Unhealthy	Purple	Health alert: everyone may experience more serious health effects.
(b)	>0.405	301 -	Hazardous	Maroon	Health warnings of emergency

- (a) Areas are generally required to report the AQI based on 8-h O₃ values. However, there are a small number of areas where an AQI based on 1-h O₃ values would be more precautionary. In these cases, in addition to calculating the 8-h O₃ index value, the 1-h O₃ index value may be calculated and the maximum of the two values is reported.
- (b) When 8-h O₃ concentrations exceed 0.374 ppm, AQI values of 301 or higher must be calculated with 1-h O₃ concentrations.

Table 2. Summary of emissions processing in the AQF system.

	Meteorologically Independent Emissions (calculated outside of the AQF system using SMOKE)	Meteorologically Dependent Emissions (calculated in the AQF system using PREMAQ)
Point Sources	Computed temporal emission fluxes.	Plume rise calculations performed hourly with merging of temporal, spatial, and speciation matrices.
Mobile Sources	Divided into exhaust and evaporative emission component sources. Computed by day of week, by hour of day, by grid cell, and by chemical species using MOBILE6. Fluxes are computed using a nonlinear least squares approximation of the relationship between MOBILE6 emission estimates and temperature from a previous time period.	Exhaust and evaporative component sources are modified with hourly temperature-dependent effects using hour, day, species, and cell-specific information for the United States only.
Area Sources	Computed emission fluxes from distributed and varied surface sources.	No meteorological dependence is considered.
Biogenic Sources	Normalized biogenic emission fluxes by species and grid cell.	BEIS3 model estimates are used in conjunction with Eta Model forecasts of temperature, radiation, and rainfall fields

for temporal and speciation of biogenic
emission estimates for each hour.

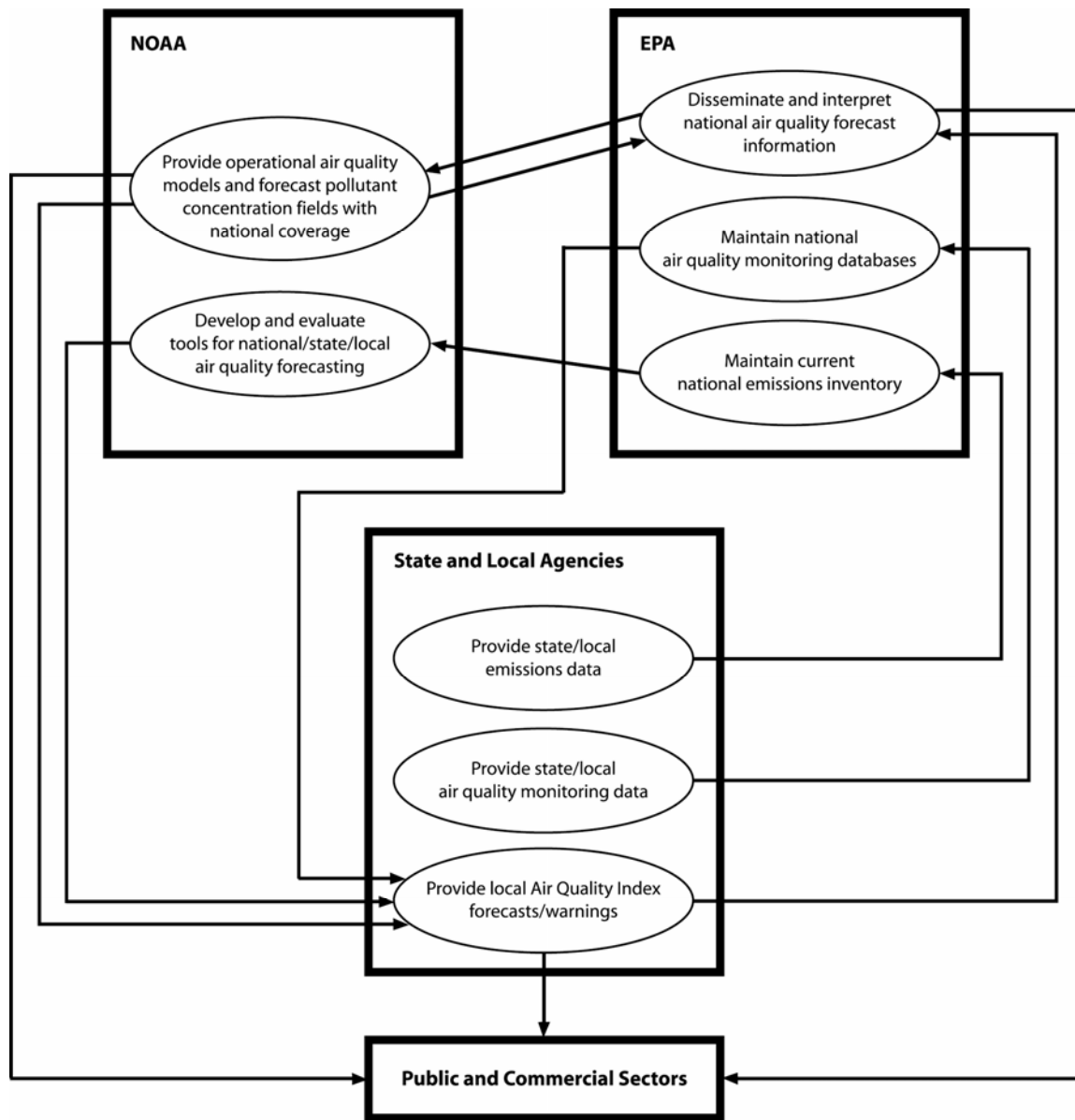


Figure 1. Roles of NOAA, the EPA, and state and local agencies in the development and execution of the air quality forecast system.

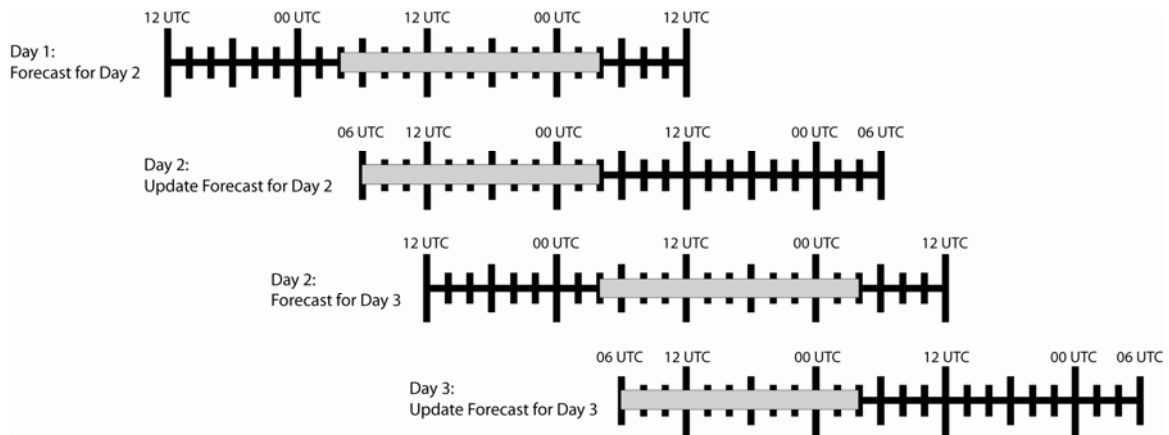


Figure 2. Operational 48-h forecast periods for the AQF system. Simulations are initialized at 0600 UTC and 1200 UTC daily. Gray bars indicate the target air quality forecast period of local midnight to local midnight, eastern daylight time.

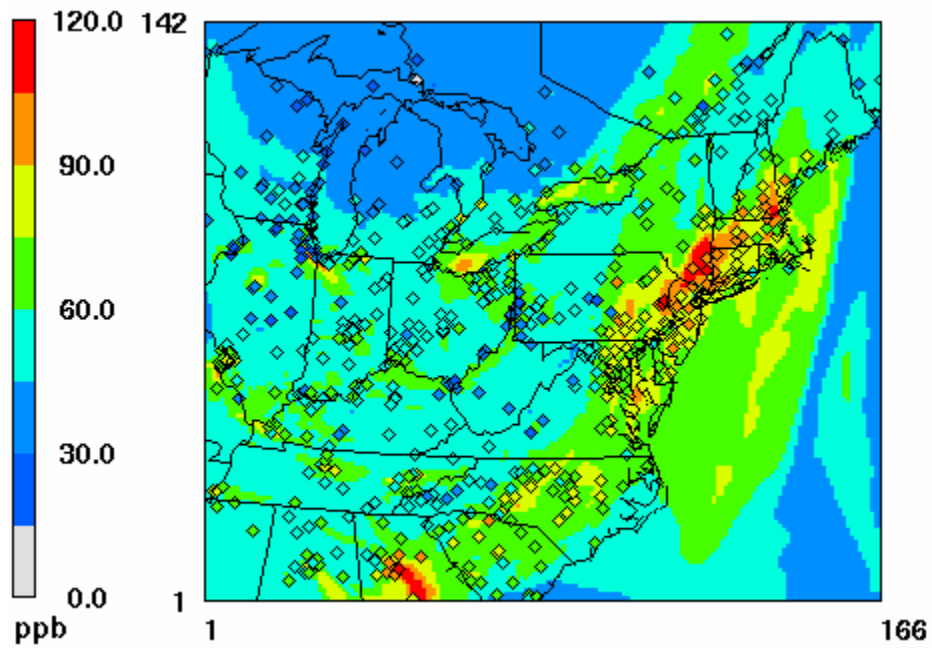


Figure 3. Forecast 1-h average surface O₃ concentration (in ppb) from the AQF system compared with observations, valid 2000 UTC 22 July 2004. The forecast was initialized at 1200 UTC 21 July 2004. The O₃ observations are overlaid in diamonds using the same color scale as the AQF system forecast. The color scale does not align with the AQI.

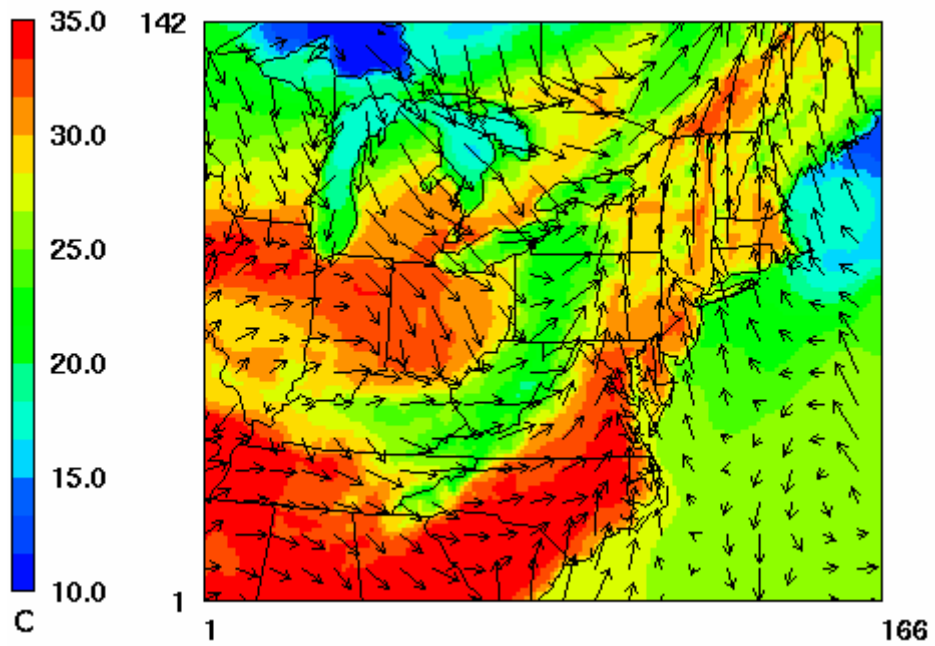


Figure 4. Forecast 2-m air temperature with near-surface wind vectors from the Eta Model, valid at 2000 UTC 22 July 2004. The forecast was initialized at 1200 UTC 21 July 2004.

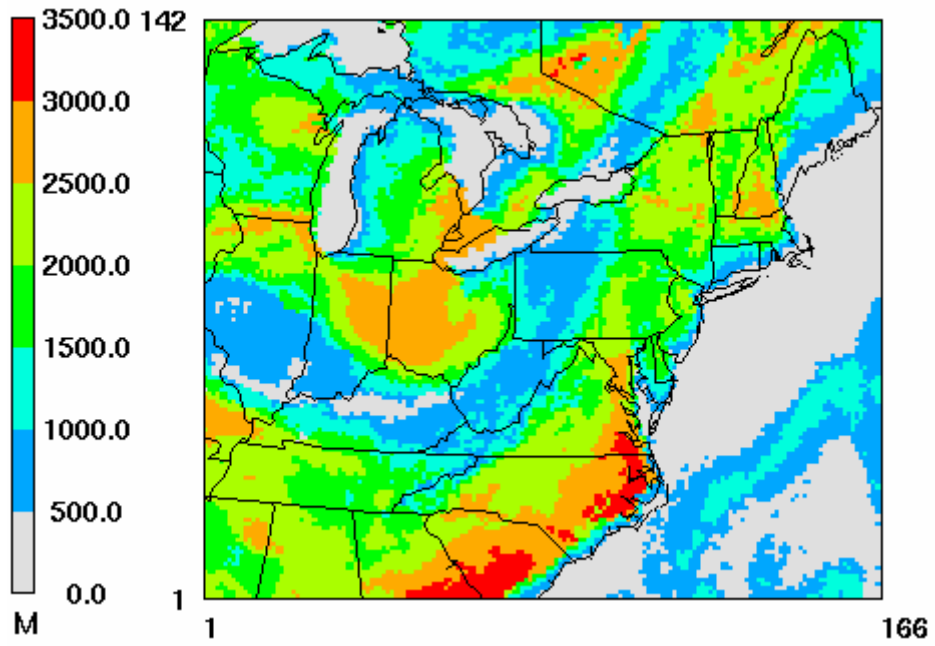


Figure 5. Forecast PBL height from the Eta Model, valid at 2000 UTC 22 July 2004. The forecast was initialized at 1200 UTC 21 July 2004.

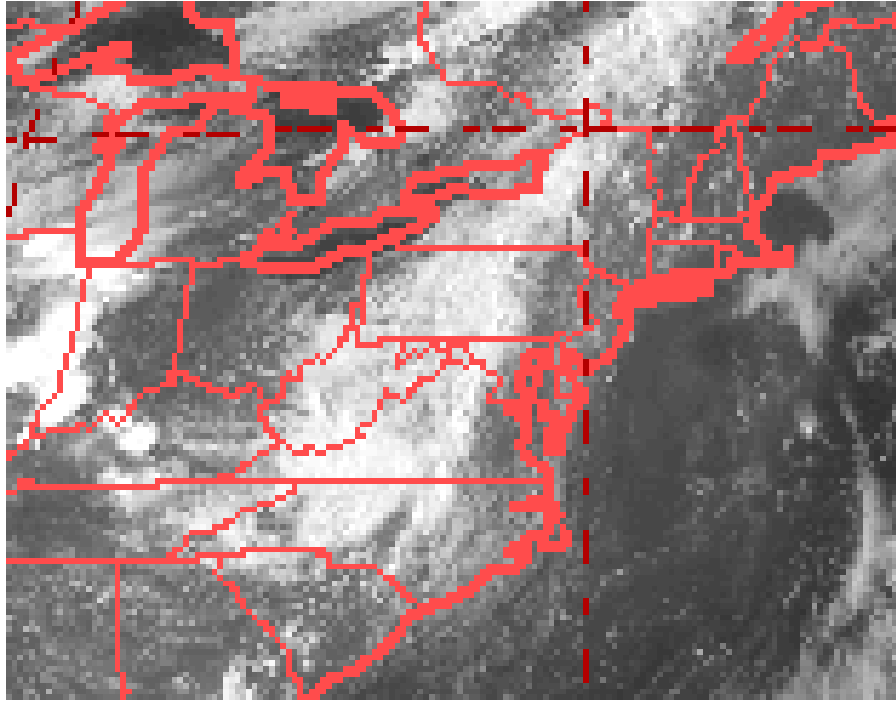


Figure 6. Cropped image from the eastern Geostationary Operational Environmental Satellite (GOES-East, which is currently GOES-12). The image is valid at 2000 UTC 22 July 2004. Original image is taken from the online archive maintained by San Francisco State University.

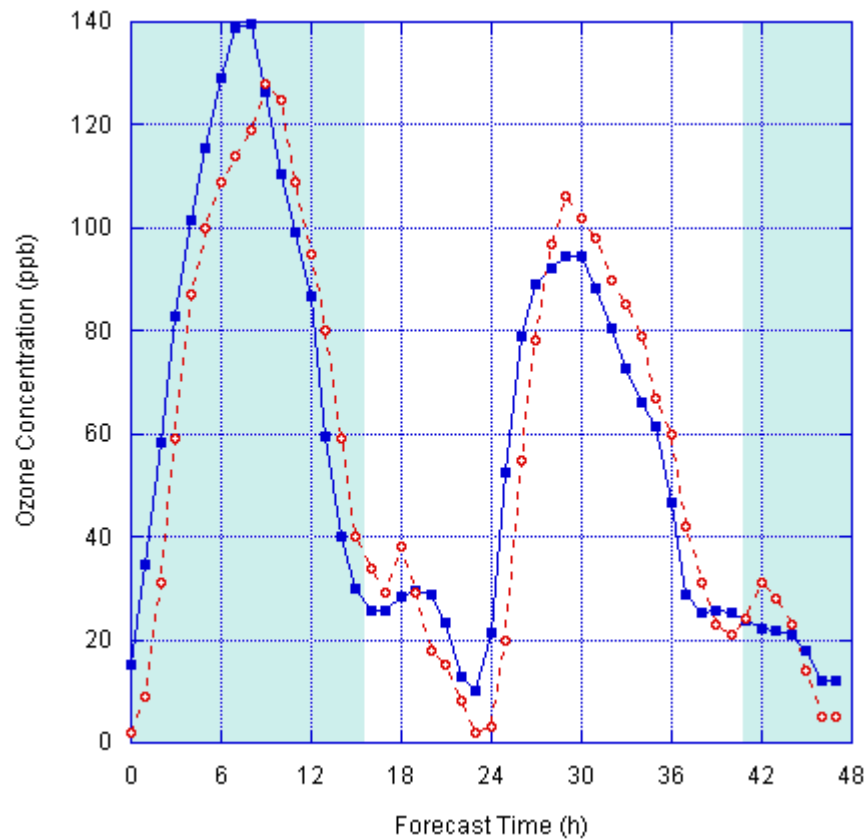


Figure 7. Forecast surface hourly O₃ concentrations (in ppb) from the AQF system compared with observations from AQS monitor 130893001 at Tucker, GA, northeast of Atlanta. The forecast was initialized at 1200 UTC 21 July 2004. The AQF system forecast is shown in squares connected with a solid line. Observations are shown in open circles connected with a dotted line. The target forecast period (0400 UTC 22 July 2004 through 0400 UTC 23 July 2004, refer to Fig. 2) is in white, while the other forecast times are shown in gray.

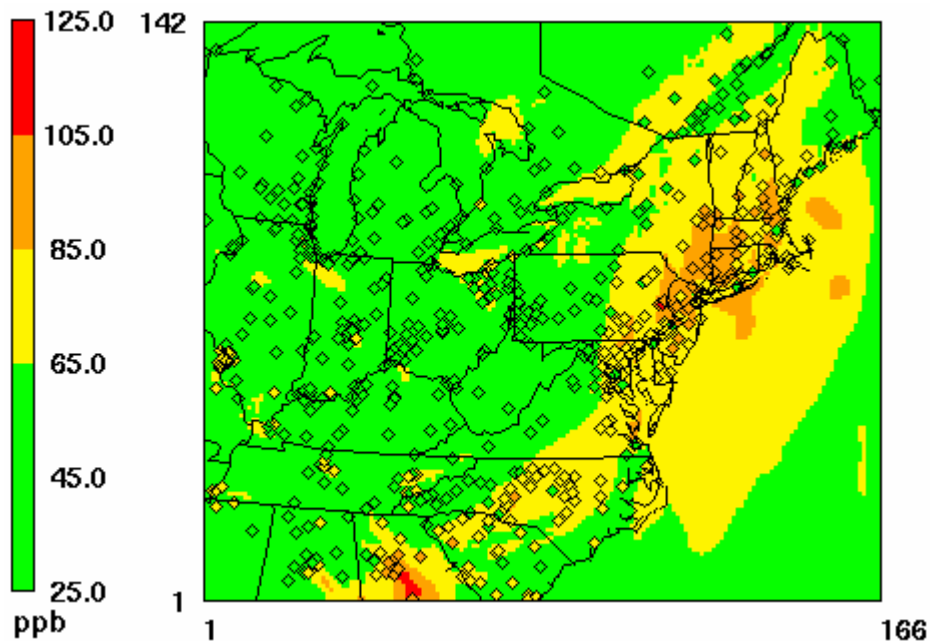


Figure 8. Forecast surface maximum 8-h average O₃ concentrations (in ppb) from the AQF system compared with observations, valid 22 July 2004. The forecast was initialized at 1200 UTC 21 July 2004, and the graphic represents the target forecast period (0400 UTC 22 July 2004 through 0400 UTC 23 July 2004, refer to Fig. 2). The observed maximum 8-h average O₃ concentrations are overlaid in diamonds using the same color scale as the AQF system forecast. The color scale aligns with the AQI categories for this pollutant.